Development of a balloon borne hard X-ray telescope using multilayer supermirror

Keisuke Tamura[a], Kojun Yamashita[a], Yuzuru Tawara[a], Yasushi Ogasaka[a], Kazutoshi Haga[a], Takashi Okajima[a], Satoshi Ichimaru[a], Seiji Takahashi[a], Hideo Kito[a], Arifumi Goto[a] Kentaro Nomoto[a], Hiroyuki Satake[a], Seima Kato[a], Hideyo Kunieda[b] Peter J. Serlemitsos[c] and Jack Tuller[c]

[a]Department of Astrophysics, Nagoya University, Furo-cho, Chikusa-ku, Nagoya
[b]Institute of Space and Astronautical Science, 3-1-1 Yoshinodai, Sagamihara, Kanagawa
[c]Laboratory for High Energy Astrophysics, Goddard Space Flight Center, Greenbelt, MD 20771

ABSTRACT

We have been developing high throughput X-ray telescope for hard X-ray region (20-40 keV) using Pt/C multilayer supermirrors for balloon borne experiment launched in 2001 June. The Walter type I telescope consists of about 2,000 supermirrors coated on very thin (150 μm) aluminum foils. We started mass production of the supermirror reflectors. Two different method is used for fabrication process. One is multilayer deposition on the platinum replica foil, and the other is direct replication of supermirror.

The performance of the supermirrors are measured in X-ray beam line in Nagoya University and synchrotron radiation facility SPring-8. We obtained 30% reflectivity at 30 keV, corresponding to 0.35 nm interfacial roughness by Debye-Waller factor. The performance of multilayer supermirrors indicate that we can achieve about 100 cm^2 effective area for a telescope.

Keywords: Balloon, Hard X-ray, telescope, supermirror

1. INTRODUCTION

The X-ray telescopes onboard previous satellites have carried out X-ray imaging observations on various X-ray objects. Because of small critical angle of the reflectors used in these telescopes, the effective energy range was limited below a few keV. Furthermore, the X-ray telescope onboard ASCA satellite[1] expand the high energy limit of X-ray imaging up to 10 keV by employing tightly nested thin foil mirrors with grazing angle 0.3 – 0.7 deg. However, as for hard X-rays more than 10 keV, the critical angle is so small that these extreme grazing optics is not suitable for practical use, because such small incident angle reduce the field of view. Therefore, hard X-ray imaging carried out with coded masks. But their image quality and background rejection capability are behind a focusing telescope by orders of magnitude.

Comparing with total reflection mirror, the multilayer can reflect the harder X-rays by using Bragg reflection. It seems to be suitable for reflectors of hard X-ray optics. However, the reflectivity of the multilayer shows very narrow peak around Bragg angle and puts constraints relation between incident angle and energy of X-ray. We introduced depth graded d-spacing multilayer, so called "supermirror", to overcome this difficulty. We can design the supermirror to cover wide energy range with flat response. Figure 1 shows the example of reflectivity curve of Pt/C supermirror with that of gold single layer and constant d-spacing multilayer. This supermirror consists of four different multilayers, the periodic length(d) and the number of layer pairs(N) are (d[nm], N) = (4.6 – 5.0, 5), (4.0, 8), (3.6, 13), (3.3, 18), each other. This supermirror shows about 40% reflectivity between 25 – 40 keV with interfacial roughness of 0.3 nm.

The balloon borne experiment using hard X-ray telescope, named InFOCμS, will be launched in 2001 June. Two hard X-ray telescope will be boarded and each telescope has about 100 cm^2 effective area between 20 – 40 keV. About two thousand reflectors are needed for each telescope, we started mass production of the supermirror reflectors. We reported present status of production of supermirror reflectors.

Further author information: (Send correspondence to Keisuke Tamura)
Keisuke tamura: E-mail: tamura@u.phys.nagoya-u.ac.jp

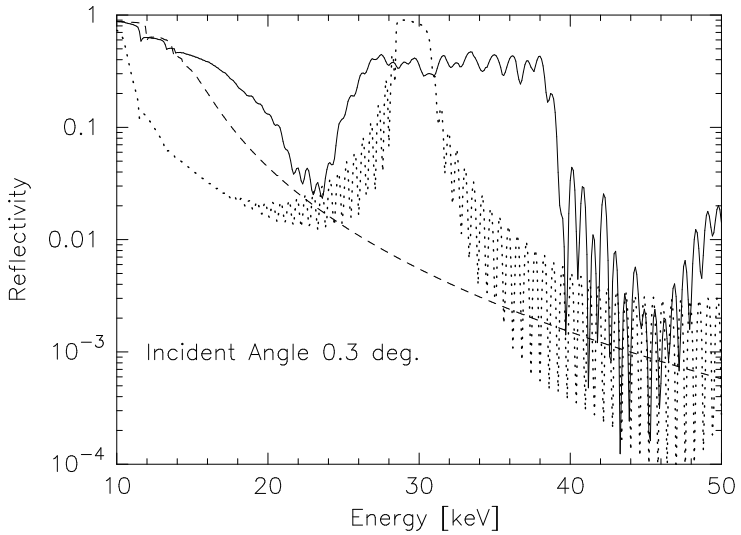

Figure 1. Comparison of three type of X-ray reflectors. All reflectivity curves calculated for grazing incident angle of 0.3 deg. Dashed line;Gold single layer, doted line;Pt/C multilayer(44 layer pairs, 4 nm periodic length), solid line;Pt/C supermirror(see text). The Γ-value are fixed 0.4, and interfacial roughness are 0.3 nm.

2. INFOCμS MISSION

The multi-nested Walter type I X-ray telescopes,[2] based on the XRT for ASTRO-E mission,[3] is developed for InFOCμS mission at NASA Goddard Space Flight Center. It has about 40 cm diameter and consists of four quadrants. About 2,000 supermirror reflectors, tightly nested in coaxial configuration, allow us to unitize more than 50% of the whole telescope aperture area, and make us possible to achieve the effective area of about 100 cm^2 between 20 – 40 keV for each telescope.

The focal length is about 8 m and the focal plane detector is multi pixel CdZnTe semiconductor detector. The spatial resolution, measured with demonstration model,[4] is 2.4 arcmin. in half power diameter (HPD). Now we trying to improve the image quality to the 1-arcmin HPD level. The field of view is determined by the design parameters of supermirrors, described in next secction. About five arcmin. field of view can be achieved by our designs of supermirrors.

The InFOCμS mission is the fruit of an international collaboration between three groups in U.S.A. and Japan;The X-ray group at NASA/GSFC for the mirror shells and housing, the X-ray group in Nagoya University for the multilayer deposition, the γ-ray group at NASA/GSFC for the CdZnTe imager, and finally a joint effort for the hard X-ray measurements at NASA/GSFC. It will be launched in 2001.

3. DESIGN OF SUPERMIRROR

Design of supermirrors have to satisfied some conditions, listed below.

1. High reflectivity for effective area of the telescope.
2. Flat and wide response for photon statics and wide field of view.
3. Small number of layer pairs to reduce the time to product X-ray reflectors.

We achieved design of supermirrors by superposing some constant d-space multilayers which have different parameters. Figure 2 shows an example of this design. Four multilayers are piled up on the substrate, and number of layer pairs of a block is increased from surface side to substrate side, to obtain flat response.

The grazing incident angles of out telescope are scattered from 0.15 to 0.35 degree. We devided them into 13 groups, and optimized the design od supermirror for each. All design parameters of supermirrors are summerized in table 1, and the reflectivity curves are shown in figure 3.

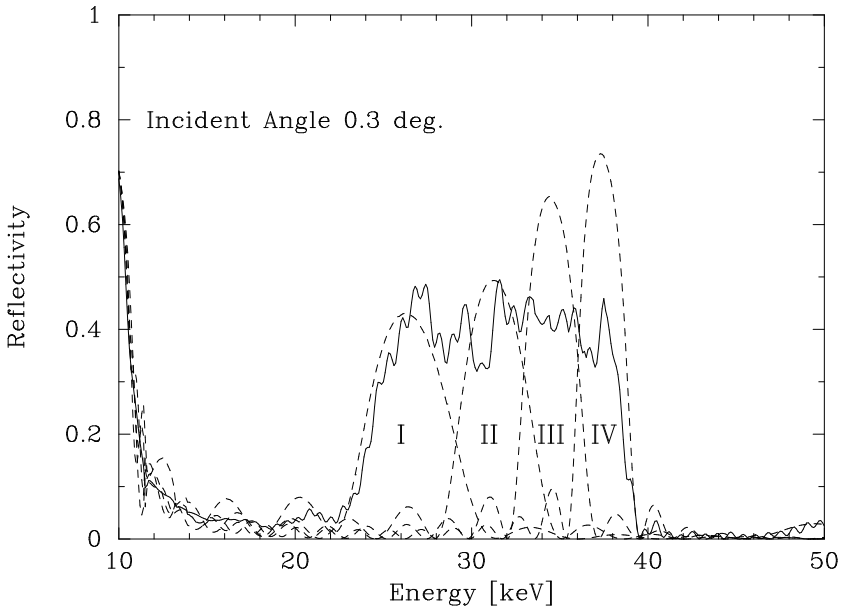

Figure 2. The reflectivity curve of four Pt/C multilayers(dashed line) and supermirror which consists from the four multilayers(solid line).

Group	Grazing Angle [deg.]	Parameters (d[nm], N)
1	0.105 – 0.125	Pt4.0 (9.0,1),(8.0,1),(7.1,3),(5.5,4),(4.9,6)
2	0.125 – 0.131	Pt4.0 (9.0,1),(8.0,1),(7.0,1),(6.5,5),(5.0,7)
3	0.132 – 0.144	Pt4.0 (8.1,1),(7.2,1),(6.5,1),(6.2,2),(5.0,4),(4.3,5)
4	0.145 – 0.158	Pt4.0 (7.2,2),(6.4,4),(5.5,6),(4.8,8),(4.3,10)
5	0.159 – 0.174	Pt4.0 (6.8,4),(5.5,6),(4.8,7),(4.1,13)
6	0.175 – 0.192	Pt4.0 (6.6,3),(5.9,4),(4.9,8),(4.3,11),(3.8,15)
7	0.192 – 0.210	Pt4.0 (6.6,2),(6.0,4),(5.1,7),(4.5,8),(4.0,9),(3.6,11)
8	0.211 – 0.232	Pt3.0 (6.3,2),(5.6,3),(5.0,5),(4.5,7),(4.0,10),(3.5,13)
9	0.233 – 0.256	Pt2.0 (6.3,2),(5.2,5),(4.5,7),(3.9,10),(3.5,12),(3.2,14)
10	0.257 – 0.281	Pt2.0 (5.4,2),(4.8,3),(4.3,4),(4.0,5),(3.7,8),(3.4,10),(3.1,18)
11	0.282 – 0.308	(5.9,2),(4.7,2),(4.4,4),(3.9,8),(3.5,10),(3.2,14),(3.0,20)
12	0.310 – 0.339	(5.7,2),(4.3,6),(3.9,3),(3.7,5),(3.6,4),(3.4,7),(3.2,13),(3.0,20)
13	0.341 – 0.356	(5.1,2),(3.9,5),(3.6,3),(3.4,5),(3.3,3),(3.2,7),(3.1,13),(2.9,22)

Table 1. Parameters of supermirror. The Γ-values are fixed to 0.4.

Total reflection play important roles when the grazing angle is less than 0.3 degree. Such small grazing angle, relatively soft X-rays don't penetrate into the deep layers. It means Bragg reflection is not so efficient around the critical energy of platinum. We used platinum top layer to 1st to 10th group of design. In figure 3, the reflectivity curves smoothly changed between total reflection region and Bragg peak. This effects on the wide energy band and wide field of view.

The total effective area of our telescope are shown in figure 4. The energy response shows flat top feature. In the case that the supermirrors have ideal interface structure, the effective area of the telescope is about 130 cm^2 at 30 keV. However, interfacial roughness of 0.4 nm reduced effective area to about 80 cm^2 at 30 keV. The vignetting curves at 6keV, 25 keV, 30 keV, 35 keV and 40 keV are shown in figure 5. From this figure, the field of view, FWHM of the vignetting curve, are 5 arcmin. at 25 keV and 3.2 arcmin. at 40 keV.

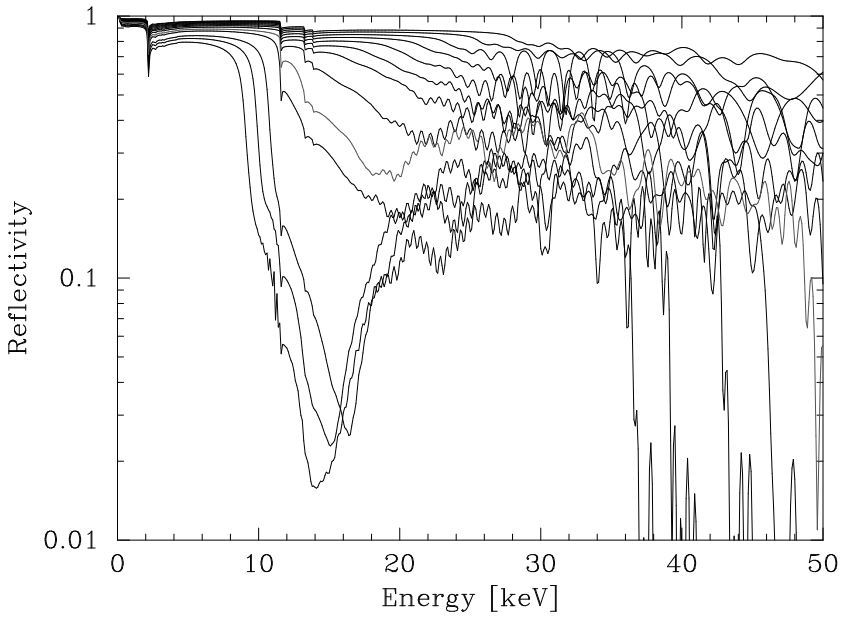

Figure 3. The calculated reflectivity curves of 13 supermirrors. The interfacial roughness are fixed at 0.4 nm.

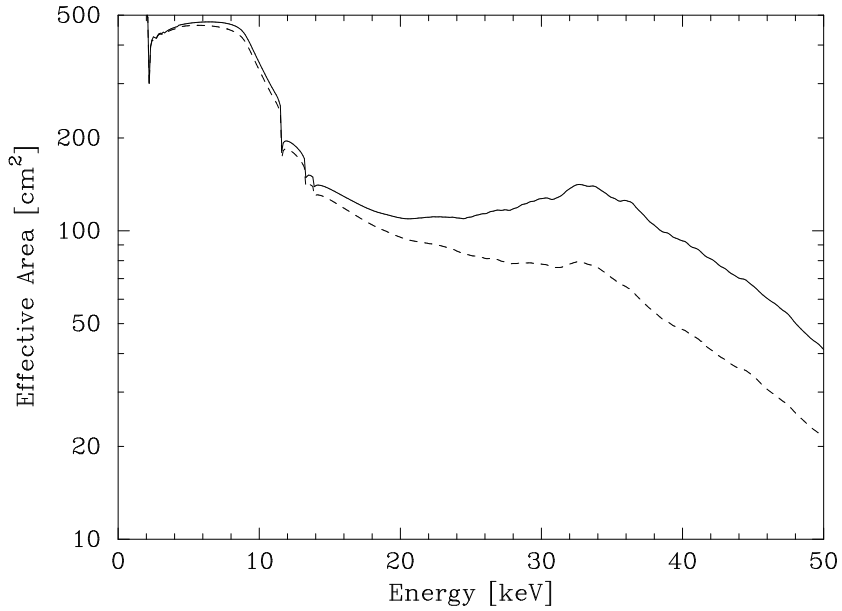

Figure 4. The calculated effective area of X-ray telescope for InFOCμS. Solid line shows effective area with ideal interface supermirrors, and break line show that with 0.4 nm interfacial roughness.

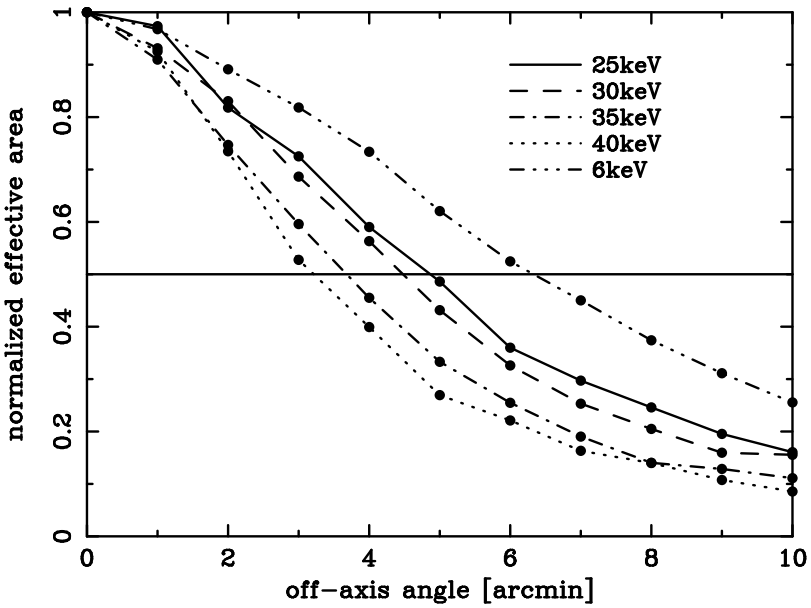

Figure 5. The vignetting curves with off axis angle at 6 keV, 25 keV, 30 keV, 35 keV, 40 keV.

4. FABRICATION OF SUPERMIRROR

We are tying to fabricate the X-ray reflectors with two methods. One is deposition on the platinum replica foil which was developed for ASTRO-E mission and provided by X-ray team in NASA/GSFC. The platinum replica foil is very thin for tightly nested X-ray telescope. It is consists of three layers including thin aluminum foil(150 μm), replicated platinum surface($\sim$150 nm) and epoxy layer($\sim$20 μm) to bond other two layers. We deposit supermirror on the smooth surface of platinum layer with DC magnetron sputter system which was specially designed to deposit onto the inner surface of cylindrical substrate. Two disk type sputter targets, platinum and carbon, located top and bottom of vacuum chamber. Samples are mounted on the stage which can move between platinum and carbon, and rotates around the targets. Masks are mounted on just front of target window for the vertical uniformity of the thickness of layers (<2%).[5] The deposition rate on the substrate surface is $\sim$ 0.1 nm/sec for platinum and $\sim$ 0.04 nm/sec for carbon. Control of thickness of layers is carried out with rotation speed. In order to avoid heat damage to the epoxy layer of Pt replica foil, temperature of foils must be kept below 50 °C. Therefor the sputter heads are cooling with water.

The other method of fabrication of reflectors is direct replication of supermirror deposited on the mandrel. This method has some advantage of the other method described above. Because the supermirror is deposited on the glass mandrel, heat damage is not serious for this method. Furthermore, we can reduce the process of fabrication with direct replication method. It is great advantage for mass production of X-ray reflector for telescope. We introduced new DC sputter system to deposit the multilayer on the mandrel. It has two square (H250 × W150 mm) sputter heads. The rotary stage is divided into four partition, and four cylindrical mandrels can be mounted on each partition. Because the targets are much longer than foil's hight (100 mm), distribution of vertical distribution of thickness is not so significant (within 3%), it make us possible to deposit the multilayer without the mask. These features make possible to deposit very fast rate compared with the other system, 1.1 nm/sec for platinum and 0.23 nm/sec for carbon.

5. MEASUREMENTS

Now we begin mass production of the supermirror reflectors for flight model. X-ray measurements of the performance of these supermirrors are carried out using X-ray beam line in Nagoya university. In addition, we used beam line in SPring-8, it is world's most powerful third-generation synchrotron radiation facility. X-ray reflectivity and scattered profile measurements are carried out mainly.

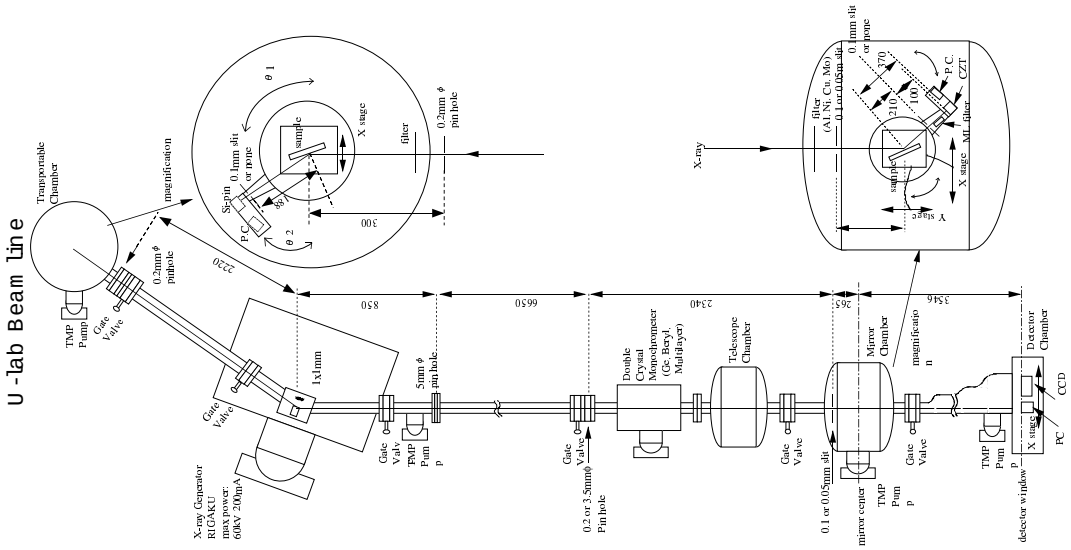

Figure 6. X-ray beam-line in Nagoya university.

5.1. Measurements Systems

Figure 6 illustrates the beam line in Nagoya university. The X-ray tube RIGAKU RU-200 (60 keV, 150mA) is X-ray source. We use Cu-Kα(8.04 keV) and Mo-Kα(17.4 keV) characteristic X-rays to measure the angle dependence of reflectivity and scattering profile. The X-rays are monochromatized with double crystal monochrometer (Si(111)) and collimated with 0.1mm pinhole. The continuum component from X-ray generator also used to measure the energy dependence of reflectivity. Samples are mounted on the θ stage and CdZnTe semiconductor detector is mounted on 2θ arm.

We also used BL24XU in SPring-8(Gap energy 8 GeV, Max current 100 mA) for the measurements of the performance in hard X-ray region. The measurements above 20 keV, where our supermirrors will be actual used, must be required. Powerful synchrotron radiation is most suitable hard X-ray source. X-rays were monochromatized with Si(111) double crystal monochrometer and collimated to size of 20 $\times$ 20 μ using tungsten slit. NaI scintillation counter was used to detect X-rays.

5.2. X-ray Reflectivity of Supermirrors

The reflectivity of the 6th and 13th group supermirror, deposited on the platinum replica foil, at Cu-Kα and 30 keV X-ray are shown in figure 7 and 8. The break lines are calculated reflectivity with 0.35 nm interfacial roughness (DW) and well fit the data. The reflectivity of 30% of 8th group suppermirror and 28% of 13th group at 30 keV is enough high to achieve 100 cm^2 effective area for a telescope.

The reflectivity of the 8th supermirror, fabricated using direct replication method, is shown in figure 9. Comparing with reflectivity shown in figure 9, there are no significant difference. The performance of supermirror fabricated using direct replication method also has enough performance for our telescope.

5.3. Scatter Profile

The scatter profile of the supermirror is very complex compared with that of single layer using total reflection. The correlated structure of the interface of multilayer called "correlated roughness", caused unspecular reflection. It is same principal with the multilayer grating. The scatter profile can be represented by convolution of depth structure of supermirror and lateral correlated structure. Accurate measurements of X-ray scatter profile must be required to construct the point spread function(PSD) of the telescope.

Figure 10 shows scatter profile of 8th group supermirror. These complex structures reflected the reflectivity profile shown in figure 7. These data are used in ray-tracing program, and we try to calculate the image quality and effect of stray light of the telescope.

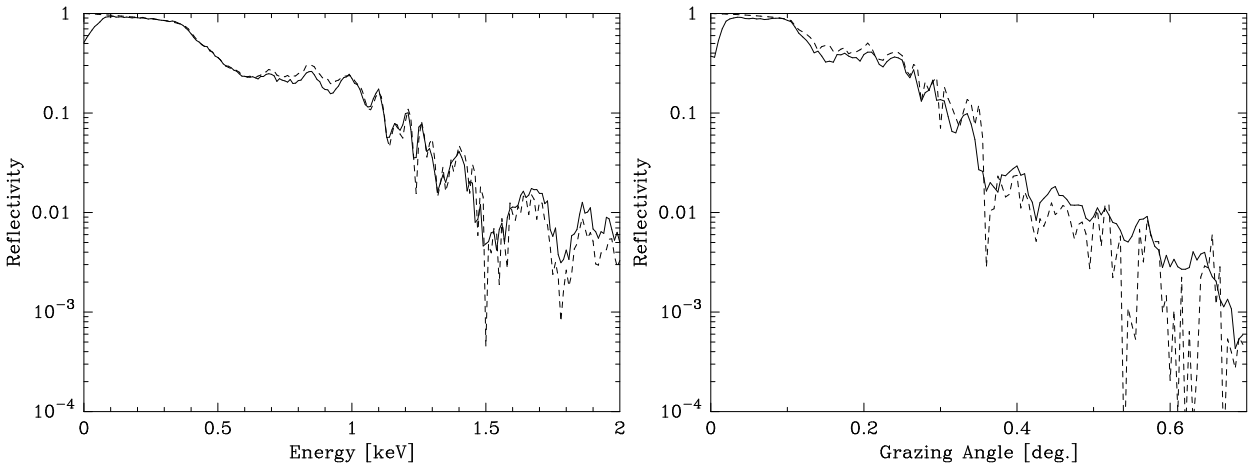

Figure 7. X-ray reflectivity of 8th group supermirror at 8 keV(left panel) and 30 keV(right panel) are shown in solid line. Break line shows calculated curves with interfacial roughness of 0.35 nm.

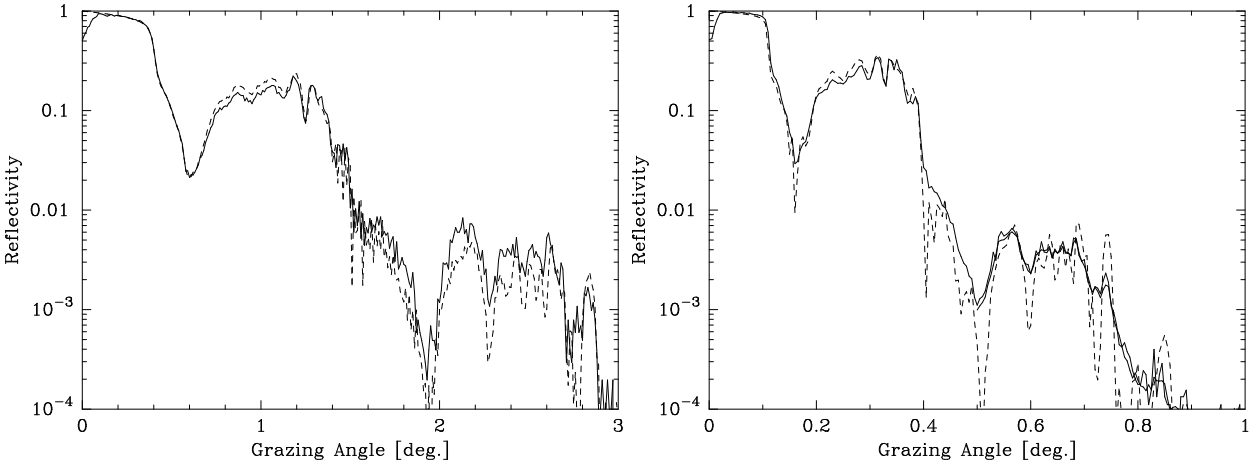

Figure 8. X-ray reflectivity of 13th group supermirror at 8 keV(left panel) and 30 keV(right panel) are shown in solid line. Break line shows calculated curves with interfacial roughness of 0.35 nm.

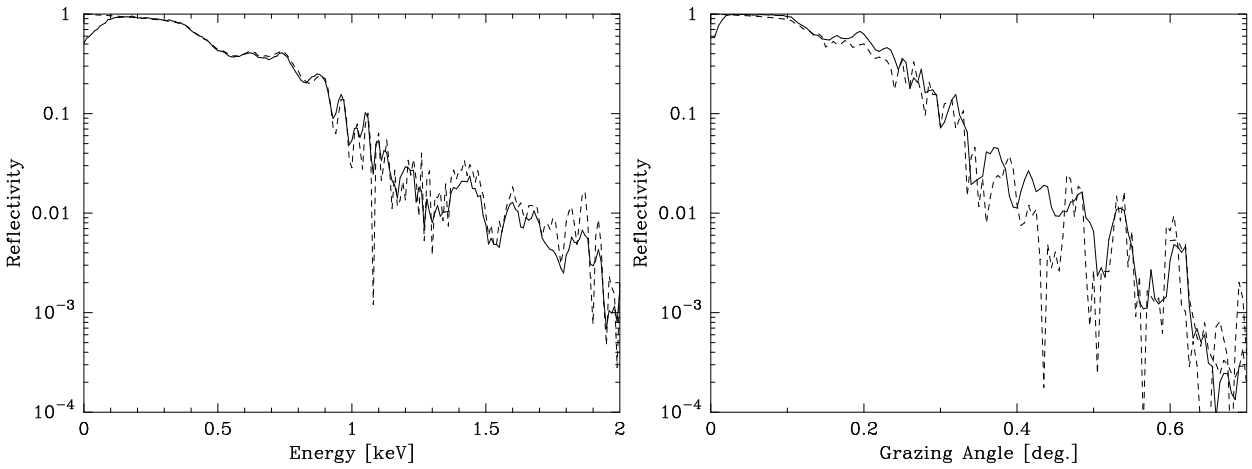

Figure 9. X-ray reflectivity of 13th group replicated supermirror at 8 keV(left panel) and 30 keV(right panel) are shown in solid line. Break line shows calculated curves with interfacial roughness of 0.30 nm.

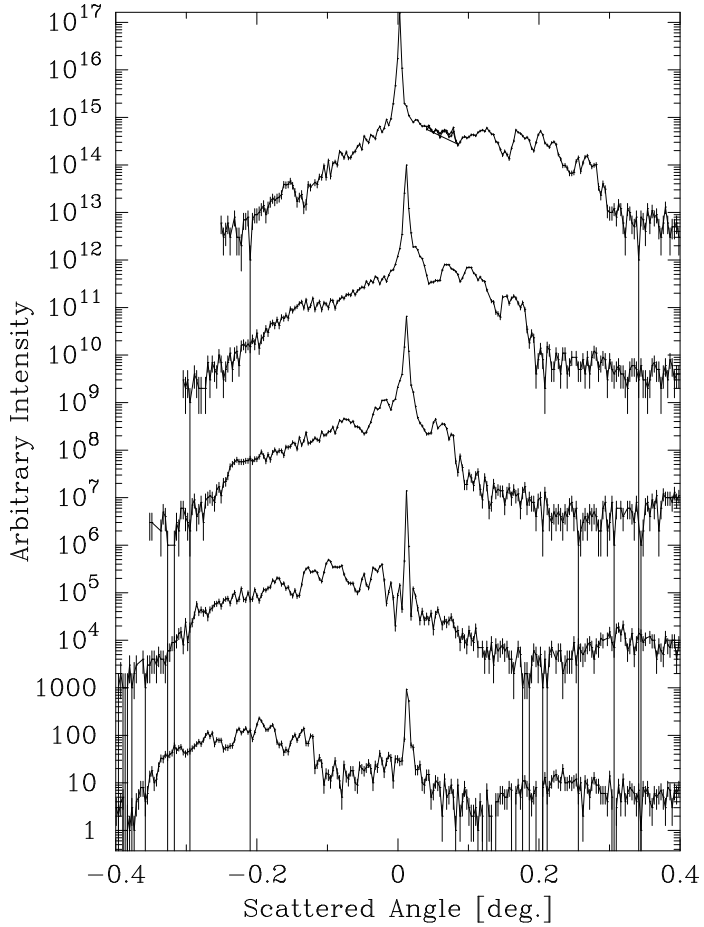

Figure 10. Scatter profile of 8th group supermirror at 30 keV. Grazing incident angles of each profiles are 0.121, 0.171, 0.221, 0.271 and 0.321 deg. respectively.

6. CONCLUSION

Our balloon borne experiment using hard X-ray telescope will be launched in 2001 June. Production of X-ray reflectors started using two fabrication methods. One is deposition on the Pt replica foils, and the other is direct replication of supermirrors. We measured these reflectors using X-ray beam line in Nagoya University and synchrotron radiation facility SPring-8. The reflectivity of 30% at 30 keV show that we can achieved about 100 cm^2 effective area for a telescope. Furthermore, scatter profile of supermirrors are obtained and used to construct the PSD of telescope.

REFERENCES

1. P. J. Serlemitsos, "The x-ray telescope onboard asca," *Publ. Astron. Soc. Jpn* **47**, pp. 105–114, 1995.
2. P. J. Serlemitsos and Y. Soong, "Foil x-ray mirrors," *Astrophys. Space Sci.* **239**, pp. 177–196, 1996.
3. H. Inoue, "The astro-e mission," in *11th Colloquium on UV and X-ray Spectroscopy of Astrophysical and Laboratory Plasmas*, K. Yamashita and T. Watanabe, eds., pp. 239–241, 1996.
4. K. Yamashita, P. J. Serlemitsos, J. Tueller, S. D. Barthelmy, L. M. Bartlett, K.-W. Chan, A. Furuzawa, N. Gehrels, K. Haga, H. Kunieda, P. Kurczynski, G. Lodha, N. Nakajo, N. Nakamura, Y. Namba, Y. Ogasaka, T. Okajima, D. Palmer, A. Parsons, a. C. M. S. Y. Soong, H. Takata, K. Tamura, Y. Tawara, and B. J. Teegarden, "Supermirror hard x-ray telescope," *App. Opt.* **37**, pp. 8067–8073, 1998.
5. K. Tamura, "Development of balloon bourne hard x-ray telescope using multilayer supermirror," in *Grazing Incidence and X-ray multilayer X-ray Optical systems*, R. Hoover and A. B. Walker, eds., *Proc. SPIE* **3113**, pp. 285–292, 1997.